Water Resources Research®

Author Contributions:
Conceptualization: E. I. Slavin, D. J. Wain, L. D. Bryant, R. G. Perkins, S. Hurley
Data curation: E. I. Slavin
Formal analysis: E. I. Slavin, D. J. Wain, S. Simoncelli
Funding acquisition: D. J. Wain, L. D. Bryant
Investigation: E. I. Slavin, D. J. Wain, L. D. Bryant, M. Amani, S. Simoncelli
Project Administration: D. J. Wain
Resources: S. Hurley
Software: S. Simoncelli
Supervision: D. J. Wain, R. G. Perkins, C. Blenkinsopp
Visualization: E. I. Slavin, D. J. Wain
Writing – original draft: E. I. Slavin, D. J. Wain

The Effects of Surface Mixers on Stratification, Dissolved Oxygen, and Cyanobacteria in a Shallow Eutrophic Reservoir

E. I. Slavin[1,2] , D. J. Wain[1,3] , L. D. Bryant[1], M. Amani[1], R. G. Perkins[4], C. Blenkinsopp[1] , S. Simoncelli[1,5] , and S. Hurley[6]

[1]Department of Architecture and Civil Engineering, University of Bath, Bath, UK, [2]Now at Drinking Water Inspectorate, London, UK, [3]Now at 7 Lakes Alliance, Belgrade Lakes, ME, USA, [4]School of Earth and Ocean Sciences, Cardiff University, Cardiff, UK, [5]Now at Dŵr Cymru Welsh Water, Newport, UK, [6]Wessex Water Services Ltd, Operations Centre, Bath, UK

Abstract Top-down surface mixers are increasingly used in drinking water reservoirs to prevent the development of stratification, control cyanobacteria, and limit sediment release of soluble manganese. A targeted field investigation enabled the discrimination of artificial mixing by surface mixers from wind and convection in a shallow (6.6 m), eutrophic drinking water reservoir. Top-down surface mixers were effective at reducing vertical temperature and dissolved oxygen gradients over a 20 m radius, within which turbulent kinetic energy (TKE) input from the mixers exceeded the maximum TKE contribution from wind and convection. Meteorological conditions appeared to have a stronger influence beyond a 60 m radius from the mixers. Near-bed velocities measured using an Acoustic Doppler Velocimeter (ADV) ~30 m north of the mixers were significantly lower when the mixers were not operating; when operating, ADV signal amplitude showed localized sediment resuspension. Cyanobacteria cell counts were high throughout the reservoir but counts of low-light adapted *Planktothrix* sp. were highest near the mixers, indicating mixer operation may improve growing conditions for *Planktothrix*. While the destratification goal of mixers was accomplished locally, the limited range of influence left >90% of the reservoir subject to diurnal stratification, anoxia, and potential internal loading of inorganic nutrients and soluble metals, restricting mixer effectiveness as an in-reservoir management technique to improve raw water quality in shallow systems.

Plain Language Summary Increasingly, top-down surface mixers are used in drinking water reservoirs to provide additional mixing so water temperatures and concentrations of dissolved oxygen (DO) are uniform throughout. This uniformity minimizes (a) the likelihood of harmful algal blooms and (b) the release of nutrients and soluble manganese from the sediments. The current lack of understanding regarding surface mixers prevents effective evidence-based management by users. Here, top-down surface mixers were turned off and on in a shallow, nutrient-rich drinking water reservoir to distinguish the effects of the mixers from natural mixing. The surface mixers were found to effectively reduce temperature and DO differences over a 20 m radius and a depth of 6.6 m. The effects of the mixers were not seen at 60 m from the mixers. Within the region of influence, the mixers added more energy to the water column than natural mixing. Sediment resuspension was observed 30 m away when mixers were on, and there was a higher prevalence of algae adapted to lower light conditions in the water column closer to the mixers. Overall, it was determined that the limited range of mixing from surface mixers in shallow reservoirs restricts their effectiveness as a tool for water quality management.

1. Introduction

Artificial mixing is a common drinking water quality management practice used in lakes and reservoirs that aims to prevent stratification, thereby reducing vertical gradients of dissolved oxygen (DO) and temperature to control cyanobacteria blooms (Visser et al., 2016) and soluble manganese concentrations (Ismail et al., 2002; Li et al., 2019). One increasingly common method is the use of top-down surface mixers, where impellers situated near the surface of the water column rotate and push a plume of well-aerated water downward. The plume displaces bottom waters and causes upwelling away from the impeller (Figure 1a), creating a circulation cell (Punnett, 1991). In principle, the circulation of the water column sustains mixed conditions and prevents the development of stratification, maintaining concentrations of DO throughout the water column, and preventing the internal loading of bioavailable nutrients and soluble metals (Wagner, 2015). The advective transport of DO through the water column by artificial circulation facilitates aerobic microbial respiration and minimizes the

Writing – review & editing: E. I. Slavin,
D. J. Wain, L. D. Bryant, R. G. Perkins,
C. Blenkinsopp, S. Simoncelli, S. Hurley

reduction and transport of metals and nutrients at the sediment-water interface and internal loading of reduced chemical species (Beutel & Horne, 1999).

However, there are limited peer-reviewed literature and industry technical reports regarding the operation of top-down surface mixers in lakes and reservoirs (e.g., Han et al., 2020; Lewis et al., 2010). Anecdotal and monitoring data from reservoirs with surface mixers highlight that complete mixing is uncommon as low DO concentrations near the sediments persist, and the extent of destratification is often limited (Wagner, 2015). For example, Lawson and Anderson (2007) assessed the range of influence of 20 axial flow pumps (type of impeller/surface mixer) in Lake Elsinore, California, where the mean depth was in the range 3–6.7 m. However, results indicated that local destratification occurred with a limited range of mixing, with horizontal velocities observed only up to 18–20 m from the pumps.

Morillo et al. (2009) proposed that impeller operation produces a plume that descends to the depth of terminal penetration, where it rebounds and intrudes laterally away from the mixer at a depth of neutral buoyancy (Figure 1b). The laterally intruding water weakens stratification away from the mixer, which enhances the effectiveness of natural mixing processes and enables the lateral transport of DO (Elliott & Swan, 2013). Lewis et al. (2010) observed weakened stratification from temperature profiles 300 m away from a surface mixer in Myponga Reservoir (average depth 15 m, maximum depth 36 m) and reported the radial velocity from the surface mixer was evident at 90 m.

The amount of water moved by a surface mixer is proportional to the size and speed of the impeller. Therefore, correct sizing and operational design of impellers are essential to successfully mix the target area and optimize efficiency (Punnett, 1991). If the flow rate is too low, mixing will be insufficient to fully mix the target volume and distribute DO through the water column (Wagner, 2015). Conversely, if the flow rate is too high, there is a risk of sediment resuspension, especially in shallow reservoirs (Chung et al., 2009). For shallow, eutrophic reservoirs, there is a much greater risk that additional energy from mixers will cause sediment resuspension. Consequently, appropriate sizing and operational design of surface mixers are essential to achieve sufficient mixing to transport DO effectively to the bottom waters to satisfy the high sediment oxygen demand (SOD; Terry et al., 2017). This risk implies that reservoir depth may be a constraining factor in the effectiveness of surface mixers and raises questions about their applicability in shallow water.

The response of a water body to naturally induced mixing depends on its morphology and meteorological forcing. Stratification in shallow, eutrophic reservoirs is less likely to be maintained for the length of the summer as they are more sensitive to variations in meteorological conditions, leading to diurnal stratification and polymictic conditions (Kerimoglu & Rinke, 2013). Mixing regimes can switch between stratified and mixed within the same day due to wind mixing or penetrative convection (Yang et al., 2018). When stratification forms in shallow, eutrophic reservoirs, the small hypolimnetic to epilimnetic volume ratio can lead to high SOD, correspondingly decreased benthic DO concentrations, and increased metal and nutrient release rates from the sediment (Kerimoglu & Rinke, 2013). Microbial respiration and oxidative processes can deplete DO concentrations near the sediments, inhibiting ammonium conversion to nitrate and causing a build-up of the ammonium pool (Harris et al., 2014). This can also lead to reduction of iron (Fe^{3+} to Fe^{2+}) and manganese (MnO_2 to Mn^{2+}), solubilizing the Mn and Fe with potential release of Fe-bound phosphorus (Wang et al., 2019). Nutrient release from the sediments may subsequently be transported to the photic zone via mixing in polymictic water bodies that can lead to increased cyanobacterial productivity and taste and odor production which, combined with metal release from the sediments, can be problematic for water treatment (Perkins et al., 2019). Theoretically, surface mixer operation in shallow reservoirs, if correctly designed, should reduce the risk of ephemeral stratification and enhance DO transport to the sediments, where demand is highest.

Many questions currently exist on the suitability, functionality, and operational effectiveness of surface mixer systems, both generally and at site-specific scales, in shallow reservoirs. Understanding how surface mixers influence hydrodynamics and water quality in drinking water reservoirs is essential to support correct management and investment decisions. The aim of this study was (a) to assess the range of influence of surface mixers in a shallow, eutrophic reservoir over a stratification season (March–October), (b) to determine the relative influence of artificial, wind-driven, and convective mixing to energy input into the reservoir, and (c) to ascertain changes in water quality due to mixers. We present one of the first in situ assessments of how the operation of surface mixers affects the hydrodynamics, turbidity, phytoplankton cell distribution, and DO concentrations within a shallow
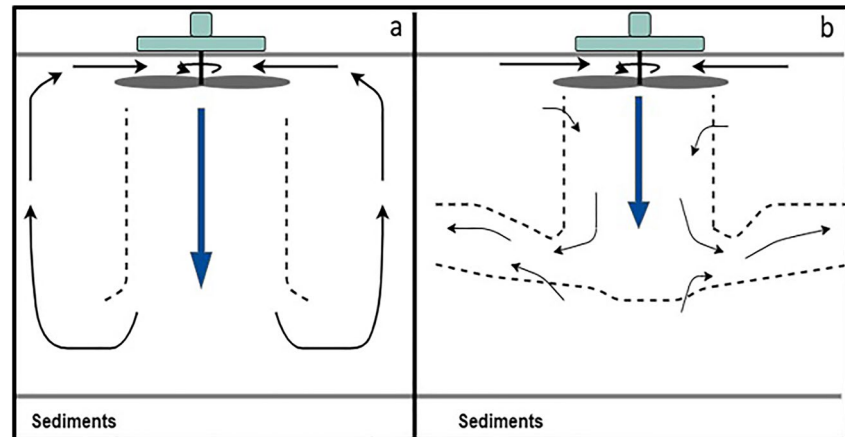
Figure 1. Two conceptual models of mixer-induced flow in reservoirs. The plume boundary is represented by the dashed line. In shallow water bodies that would naturally not maintain stratification through the summer, flow pattern (a) is expected. In deeper lakes that would naturally be stratified through the summer, flow pattern (b) is expected.

reservoir, and consider the implications for the raw water quality. By manipulating mixer operations, we were able to identify and characterize natural mixing versus mixer-induced effects on destratification and water quality. Our results extend knowledge on surface mixer operation as an artificial mixing technique and the potential water quality impacts, both intended and unintended, of using mixers in shallow eutrophic reservoirs.

2. Materials and Methods

2.1. Study Site

Durleigh Reservoir is a small (surface area: 0.33 km^2), shallow, eutrophic, lowland drinking water reservoir located near Bridgwater, Somerset, UK. It is owned and managed by Wessex Water (WW). While advanced water treatment methods are used at the works, three co-located surface mixers (Figure 2b) were installed as an in-reservoir technique in 2015 to improve the sustainability of treatment and reduce costs to consumers. At full capacity, the mean depth of the reservoir is 3.1 m and the maximum depth is 8.1 m. There are two main inflows, a natural river inflow from Durleigh Brook at the western end of the reservoir that dries up in the summer, and an intermittent pumped inflow with water taken from the Bridgwater and Taunton canal that enters the reservoir on the south side (Figure 2). In 2018, water was pumped from the canal from July 11, 2018 and continued for the duration of the study period, which ended on October 5, 2018. At full capacity (1,005,000 m^3), the residence time of the reservoir is approximately 100 days. The intake is located, at the dam wall on the east side of the reservoir and operated depending on demand, with a maximum works throughput of around 12 ML per day. The surface mixers are positioned near the intake, in the east of the reservoir (Figure 2). At full capacity, the water depth at the location of the surface mixers is ~6.6 m (Figure 2a). Each mixer has a diameter of 2.4 m and an initial plume velocity of 0.15 m s^{-1} (WEARS Australia, 2019). The surface mixers do not have draft tubes fitted. The surface mixers are adjustable but are generally operated at 0.67 m^3 s^{-1} (maximum flow rate for each mixer).

2.2. Methods and Equipment

Most data presented here are from a campaign conducted between February 22 and October 5, 2018 at three sampling locations (L1, L2, and L3; Figure 2a) with increasing distance from the surface mixers (25, 60, and 435 m away, respectively) to assess the spatial extent of artificial mixing. WW also had a monitoring buoy (B1; Figure 2a) for temperature and DO ~20 m from the mixers. During the campaign, the mixers were deliberately shut down on four occasions; however, data was only collected during three of these. The shutdowns were considered controls to determine the effects of the mixers. The first shutdown (SD-1) began at 08:00 local time (LT) on June 20, 2018 and lasted for 54 hr. The second shutdown (SD-2) began at 07:00 LT on August 22, 2018 and lasted for 34 hr. The third shutdown (SD-3) began at 06:30 LT on September 6, 2018 and lasted for 13 days, 6.5 hr. SD-1 and SD-3 were conducted by WW to facilitate maintenance work. SD-2 was planned to facilitate 5 days of more
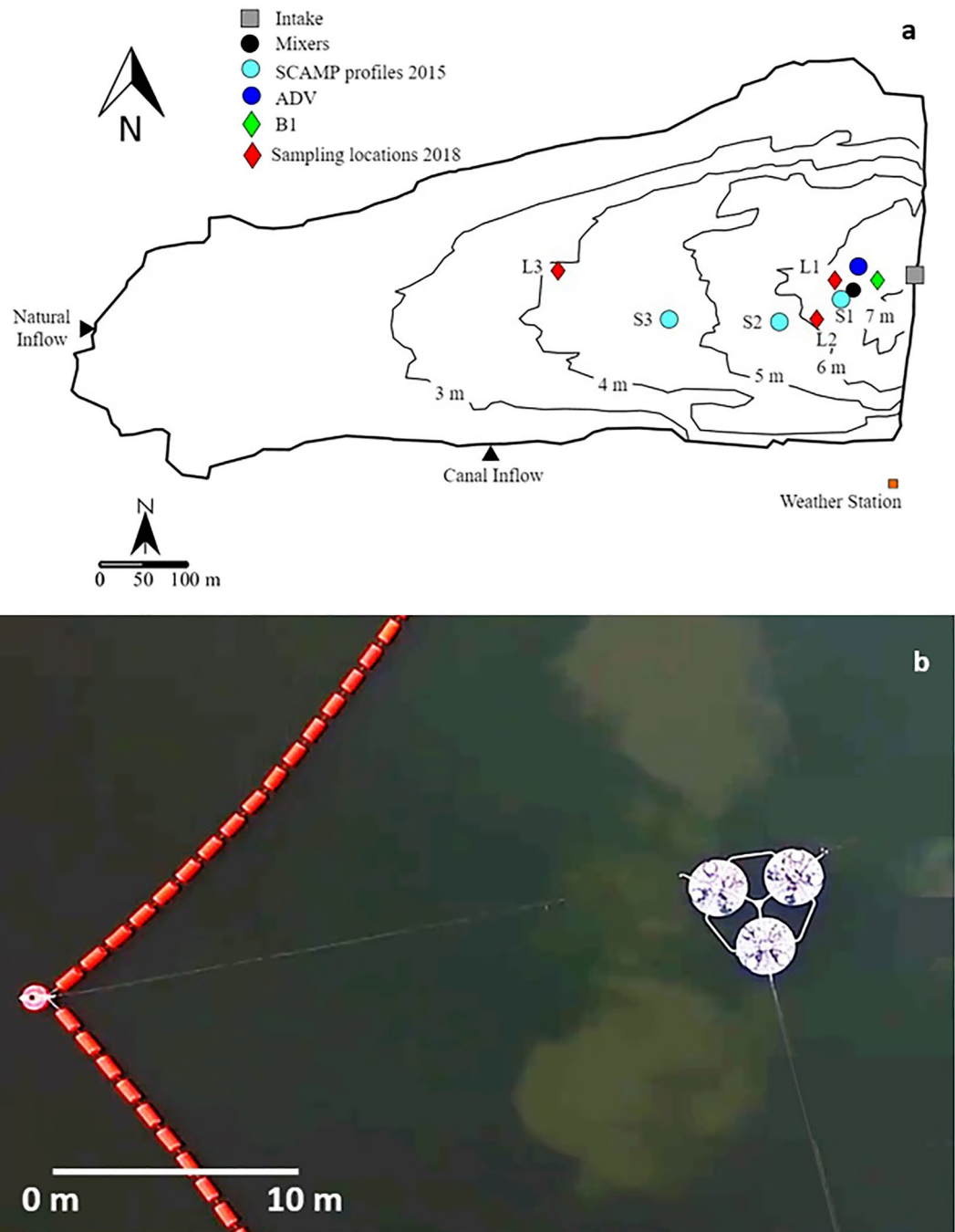
Figure 2. (a) Map of study site showing the 2018 sampling locations. (b) Aerial photograph of the surface mixers at the study site; clouds of resuspended sediment are visible around each of the mixers. Source: Wessex Water, 2016.

intensive field investigations before, during, and after the mixers being turned off. Before SD-1, three mixers were operating and after SD-1 only two mixers were operational.

To aid comparison between on and off periods around SD-1 and SD-2, an equivalent number of hours either side of the shutdown time were taken as the ON period before (B) and after (A). For SD-3, this was not possible and instead the ON periods before and after SD-3 were 12 days and 6.5 hr (the maximum time possible without overlapping with ON-A2). Comparisons between the pre-shutdown periods (hereafter ON-B1, ON-B2, and ON-B3 before shutdowns SD-1, SD-2, and SD-3, respectively), shutdown periods (SD-1, SD-2, and SD-3), and

post-shutdown periods (ON-A1, ON-A2, and ON-A3 after shutdowns SD-1, SD-2, and SD-3, respectively) were made to determine the physical impact and the range of influence of the surface mixers. Regular water sampling was conducted on February 22, April 5, April 20, May 30, June 13, June 27, July 9, July 24, and October 5, 2018 at L1, L2, and L3 (Figure 2). An intensive sampling campaign was conducted August 20–24, in the days before and after SD-2. The maximum water depth during this campaign was 6 m. During SD-1, a silt curtain was installed close to the intake to the treatment plant and one of the mixers was moved inside the silt curtain. In addition to the 2018 seasonal data, a short field campaign was conducted in September 2015 where turbulence profiles were collected from three locations (S1, S2, and S3; Figure 2a) of increasing distance from the mixers. Details of the methods used to estimate the dissipation rate of turbulent kinetic energy (TKE; ε) and vertical eddy diffusivity (K) are given in the Supporting Information of this study. The direct turbulence measurements and subsequent estimates facilitate our discussion in Section 4. During the 2015 campaign, only one mixer was operational, so the measurements presented here are used as supporting evidence of the range of mixing effects.

2.2.1. Weather and Mixing Inputs

Natural mixing in lakes is typically dominated by wind and convection from night time cooling. For comparison with the energy input from the mixers, we assessed the transfer of energy through the surface boundary layer from the atmosphere. To this end, a Delta T WS-GP1 weather station was installed on-site (on April 5, 2018) to measure wind speed and direction, rainfall, humidity, solar radiation, and air temperature. Text S3 and Table S2 in Supporting Information S1 detail the accuracy and measuring interval of the sensors. The weather station was positioned ~4 m above the water surface and located on the south bank adjacent to the dam (Figure 2a). Data were averaged hourly and input into Lake Heat Flux Analyzer (LHFA; Woolway et al., 2015). From the observations, LHFA hourly calculates the roughness lengths for momentum, heat, and moisture, the corresponding transfer coefficients, and the surface fluxes for momentum, sensible heat, and latent heat (ibid.). Because LHFA does not take into account the surface wave state, the wind shear velocity u_* was computed separately from the wind speed data following the relationships for low and high wind speeds in lakes from Wüest and Lorke (2003). TKE input from the wind (TKE$_{wind}$) was then calculated as

$$TKE_{wind} = \frac{1}{2}\rho_w \left(C_N u_*^3 \right) \tag{1}$$

where C_N (the coefficient related to wind energy utilisation for turbulent mixing) = 1.33 (e.g., Saber et al., 2018). TKE input from convection (TKE$_{conv}$) was calculated as

$$TKE_{conv} = \frac{1}{2}\rho_w w_*^3 \tag{2}$$

where $w_* = (-\beta Z_{mix})^{\frac{1}{3}}$ is the vertical convective velocity, in which β is the buoyancy flux and Z_{mix} is the depth of the mixed layer, which was determined from the thermistor chain at L2 which had RBR Solo T thermistors (manufacturer: RBR Global) placed every meter through the water column. The mixed layer depth was defined as the depth at which there was >1°C difference between thermistors (Gray et al., 2020; Mackay et al., 2011). The buoyancy flux is:

$$\beta = \frac{g\alpha H_*}{C_{\rho w}\rho_w} \tag{3}$$

where:
g = gravitational constant
α = coefficient of thermal expansion of water
H_* = net heat flux into the lake surface (from LHFA)
$C_{\rho w}$ = specific heat of water

The uncertainty in TKE$_{wind}$ and TKE$_{conv}$ were estimated by propagating the measurements uncertainty through the calculations.

Following the scaling for an axial flow pump in a lake from Imboden (1980), the theoretical TKE input into the water column from a surface mixer (TKE$_{mix}$) can be estimated as

$$TKE_{mix} = \frac{1}{2}\rho_w U_p^3 \tag{4}$$

where TKE$_{mix}$ is the TKE input from the operation of the surface mixers over the area of the mixers and U_p is the flow velocity generated by the mixers. Note that this energy input is per unit area of the mixers. The depth of penetration of the plume H_p was estimated as

$$\frac{H_p}{D} = 0.176\frac{U_p^2}{g(\Delta\rho/\rho_0)} + 0.756\frac{Z_{mix}}{D} \tag{5}$$

where D is the pump diameter, and $\Delta\rho$ is the density difference between top and bottom (Punnett, 1991).

2.2.2. Temperature and Dissolved Oxygen

Temperature measurements were obtained every 10 min from the surface and bottom of the water column at L2 (6 m) and L3 (4 m) using RBR SoloT thermistors and HOBO TidbiT v2 loggers (manufacturer: Onset). Table S1 in Supporting Information S1 gives details of the locations, accuracy, and sampling interval for the temperature measurements. L1 and B1 were similar distances from the mixers; a telemetered monitored buoy at B1 had YSI EXO sondes permanently moored at the surface and bottom providing the temperature and DO data every 15 min. Obvious erroneous data (e.g., negative temperature values) were removed and water temperature measurements from B1, L2, and L3 were averaged hourly.

For each location, Relative Thermal Resistance to Mixing (RTRM) values were calculated to assess the effects of the mixers on water column stability. RTRM is a dimensionless index that is used to define the strength of thermal stratification, and was calculated following Wetzel (2001):

$$RTRM = \frac{\rho z_2 - \rho z_1}{\rho_4 - \rho_5} \tag{6}$$

where ρz_2 and ρz_2 refer to the water densities at the bottom and surface of the water column, respectively (kg m^{-3}), and ρ_4 and ρ_5 are water densities at 4 and 5°C, respectively (kg m^{-3}).

The flux of DO between the atmosphere and the water column was computed as

$$F = k(DO_{sat} - DO_{obs}) \tag{7}$$

where k is the transfer velocity, DO$_{sat}$ is the saturation DO at the observed surface temperature, and DO$_{obs}$ is the observed surface DO. DO flux can result from both convection and wind mixing and the processes have different transfer velocities. The transfer velocity for wind was estimated for lakes following Wanninkhof et al. (1991) as $k_w = 0.108U_w^{1.64}(Sc/600)^{0.5}$ where U_w is the wind speed at 10 m and Sc is the Schmidt number for oxygen (500). Following Read et al. (2012), the transfer velocity for convection was estimated as $k_c = 0.29(\varepsilon_c v)^{0.25}Sc^{-0.5}$ where ε_c is the near-surface turbulence from convection approximated by $-\beta$ and ν is the kinematic viscosity of water.

2.2.3. Light Penetration

The SCAMP used in September 2015 was fitted with a Li-Cor LT-192SA underwater radiation sensor and profiles of Photosynthetically Active Radiation (PAR) were acquired. The euphotic depth (Z_{eu}) was estimated from these profiles as the depth at which 1% of the PAR from the surface remained. Although the SCAMP PAR profiles provide an accurate estimate for Z_{eu}, these profiles were only collected over a few days in September 2015 and therefore Secchi Disk measurements from 2018 were also used to estimate Z_{eu} following Luhtala and Tolvanen (2013):

$$Z_{eu} = m \times Z_{SD} \tag{5}$$

where the conversion coefficient (m) used was 2.5 (Dokulil & Teubner, 2003; Lindenschmidt & Chorus, 1998).

2.2.4. Flow Velocities

Near-bed flow velocities were measured using a Nortek Vector Acoustic Doppler Velocimeter (ADV) during SD-2. Installed on a stainless-steel frame, the ADV was deployed approximately 30 m north of the surface

mixers (Figure 2a) at 4.5 m water depth. The sensor was positioned to measure velocities ∼10 cm above the sediment. Prior to deployment, the ADV compass was calibrated and the instrument was set up to measure in the ENU directions. Velocities were measured using burst mode, measuring every 10 min at a frequency of 64 Hz for 1,024 samples. Signal amplitude from the ADV was used to evaluate relative levels of suspended sediment (Chanson et al., 2008). For example, clear water typically returns a weaker signal, whereas turbid water returns a stronger one (Ha et al., 2009). The ADV was deployed at 3 p.m. local time on August 20, 2018 and measured for approximately 90 hr. The results of the ADV deployment are presented in Text S4 and Figure S2 in Supporting Information S1.

2.2.5. Phytoplankton Cell Counts

Water samples were collected from the surface, middle, and bottom of the water column on sampling days in 2018 using a Van Dorn sampler, transferred to 1 L PET bottles, fixed with Lugol's iodine solution (1%), and then concentrated by membrane filtration, using 47-mm diameter cellulose acetate membranes with a pore size of 0.45 μm. The filtered membranes were then dried in an oven at $35 \pm 5°C$. Identification and enumeration were conducted using an Olympus BH2 light microscope (40× objective). The average colony and filament size were noted by measuring 10 colonies or filaments. A minimum of 15 fields of view (FOV) were counted per sample, or at least 500 cells for the most abundant genera (Lund et al., 1958).

2.3. Statistical Data Analysis

Data were analyzed using the PAST statistical software package (Hammer et al., 2001). Normality and equal variance were assessed using the Shapiro-Wilk and Levene's tests. Normal data were assessed for significant differences using single-factor ANOVA and post hoc Tukey's test. The Kruskal-Wallis test and Dunn's multiple comparison test were used for non-normal data.

3. Results

3.1. Weather and Mixing

Between April 5 and October 5, 2018, the hourly average air temperatures were in the range 2.2–29.3°C (Figure 3a) and the hourly average wind speeds were in the range 0.3–9.6 m s^{-1} (Figure 3c). Hourly average net surface heat flux (from LHFA) is presented in Figure 3b; positive values are indicative of stratifying conditions, whereas negative values reflect mixing conditions. During SD-1, the mean net heat flux at the surface was −19 W m^{-2} and the mean wind speed was 3.8 m s^{-1}, yielding a mean TKE$_{conv}$ of 1.7×10^{-4} W m^{-2} and a mean TKE$_{wind}$ of 0.9×10^{-4} W m^{-2}. During SD-2, the mean net heat flux at the surface was 47 W m^{-2} and the mean wind speed was 2.4 m s^{-1}, yielding a mean TKE$_{conv}$ of 0.6×10^{-4} W m^{-2} and a mean TKE$_{wind}$ of 0.5×10^{-4} W m^{-2} during SD-3, the mean net heat flux at the surface was 23 W m^{-2} and the mean wind speed was 2.0 m s^{-1}, yielding a mean TKE$_{conv}$ of 0.7×10^{-4} W m^{-2} and a mean TKE$_{wind}$ of 0.3×10^{-4} W m^{-2}. For the entire data record, the mean TKE$_{wind}$ was 0.5×10^{-4} W m^{-2} and was in the range 2.0×10^{-6} and 1.9×10^{-3} W m^{-2} (Figure 3d). The maximum TKE$_{wind}$ occurred on May 2, 2018, when the hourly average wind speeds were highest (9.6 m s^{-1}). The mean TKE$_{conv}$ was 0.8×10^{-4} W m^{-2} with a maximum of 6.0×10^{-4} W m^{-2} on June 21, 2018, during SD-1 (Figure 3d).

The average uncertainty in TKE$_{wind}$ was 11%, largely due to uncertainty in the wind speed. The average uncertainty in TKE$_{conv}$ was 56%, mostly due to potential inaccuracy in air temperature measurement ($\pm 0.3°C$) which influences the components of the net heat flux, and the mixed layer depth (due to the 1 m thermistor spacing). The time series of the uncertainty magnitude is shown for the net heat flux and total TKE in Figures 3b and 3e. For the net heat flux, the largest uncertainty came from the solar radiation measurements; because most convective mixing in lakes happens at night, this source of error was not significant for TKE$_{conv}$.

TKE$_{mix}$ was 1.7 W m^{-2} and was 3–4 orders of magnitude higher than combined TKE$_{wind}$ and TKE$_{conv}$ per unit area. The average estimated penetration depth of the mixer plume was 6.4 m (water depth at mixers was 6.6 m).
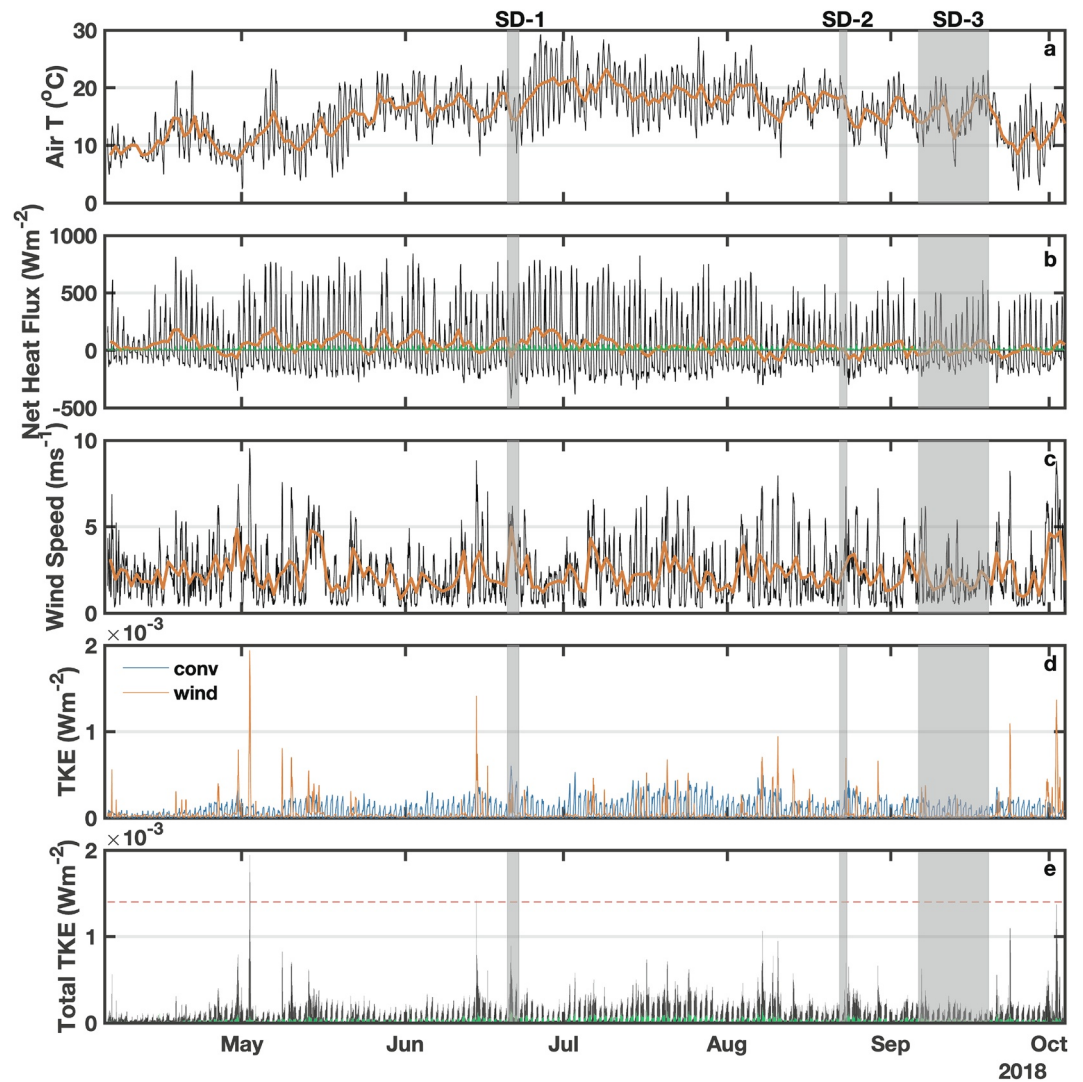
Figure 3. Hourly average (a) surface air temperature, (b) net surface heat flux, (c) wind speed, (d) TKE$_{conv}$ (blue) and TKE$_{wind}$ (orange), and (e) combined TKE from wind and convection at Durleigh between April 5 and October 5, 2018. For panels (a)–(c), the 24-hr average is overlaid in orange. In panels (b) and (e), the bars indicate the magnitude of the uncertainty based on measurement accuracy. In panel (e), the dashed red line indicates the minimum TKE contribution from two mixers distributed over the area of influence (see Section 4.4).

The mixer plume penetrated to the bottom of the reservoir 78% of the time. The minimum plume penetration depth was 2.6 m, occurring on May 21, 2018.

3.2. Temperature

RTRM indicates the intensity of thermal stratification. Values over 30 are considered to indicate that the water column is stable and values over 80 suggest there is a very strong resistance to mixing (Wagner, 2015). RTRM values from the hourly average water temperatures indicate that the mixers helped to maintain a more uniform water column at B1 (Figure 4a), as the RTRM values largely remained below 30 and always remained <80.

With increasing distance from the mixers, RTRM values of 30 and 80 were exceeded more frequently and diurnal patterns of RTRM were observed at both L2 and L3 throughout 2018 (Figures 4b and 4c). RTRM calculated at L1 exceeded 30 in 9.1% of all measurements and exceeded 80 in 0.2% of measurements. At L2, RTRM values exceeded 30 and 80 in 27.1% and 1.5% of measurements, respectively. At L3, RTRM exceeded 30 in 34.3% of
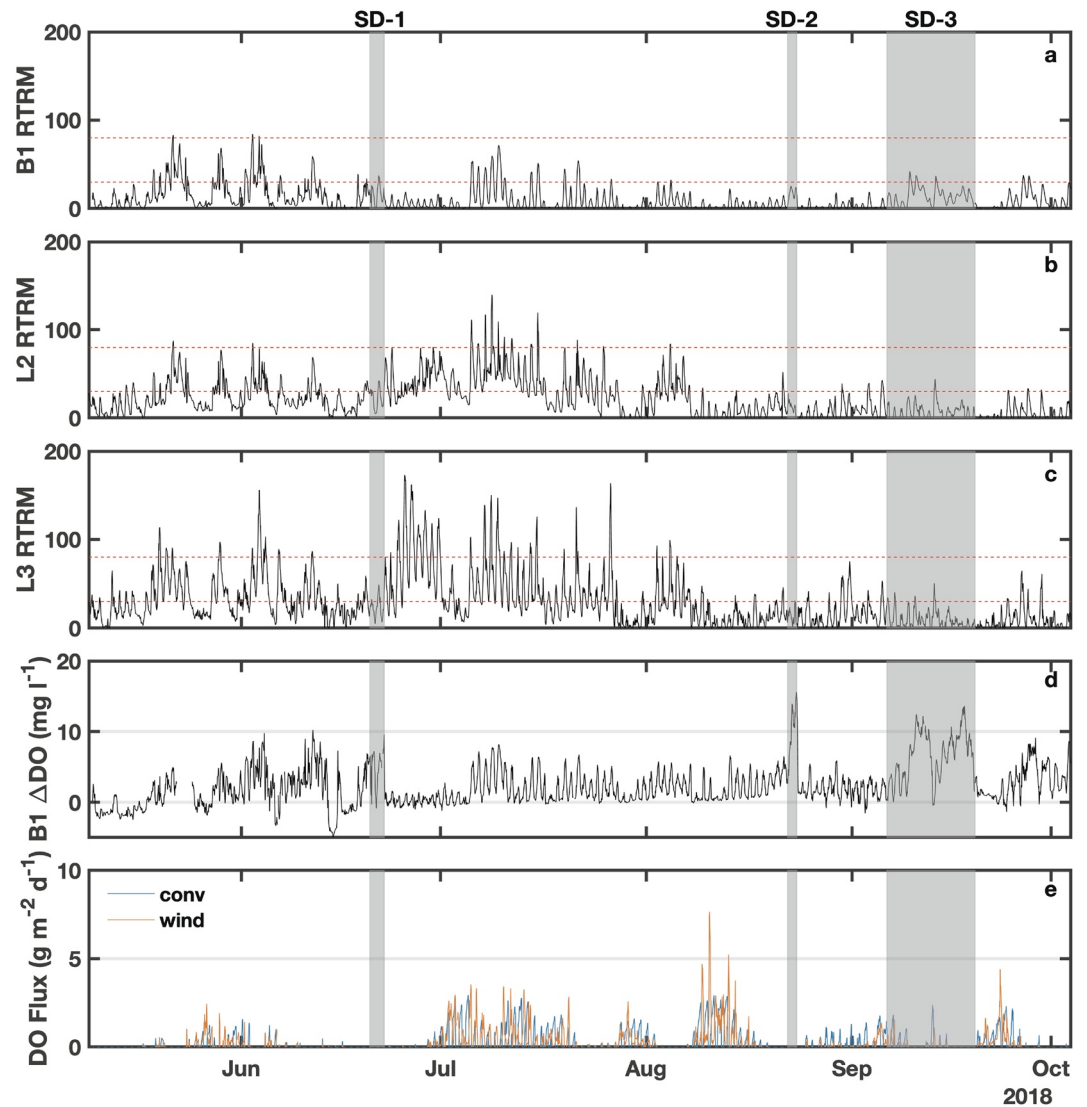
Figure 4. Relative thermal resistance to mixing (RTRM) using hourly averaged temperature data between May 9 and October 3, 2018 for (a) B1, (b) L2, and (c) L3. The red dashed lines indicate RTRM values of 30 (considered stable) and 80 (considered very resistant to mixing). (d) The dissolved oxygen (DO) difference (ΔDO) between the hourly average surface and bottom DO concentrations from B1 over same period. (e) DO flux from the atmosphere into the reservoir due to convection and wind.

measurements and exceeded 80 in 6.3% of measurements, suggesting that the shallower water column experienced more intense diurnal stratification.

Temperatures near the sediments at B1 were significantly higher than those at L2 and L3 through 2018 ($H = 1172$, $p < 0.001$, df = 2). However, bottom water temperatures at L2 and L3 were not found to be significantly different ($p = 0.09$). Surface water temperatures were found to be significantly different between all sites ($H = 758.4$, $p < 0.001$, df = 2), with L3 having the highest average surface water temperatures.

At site B1, shutdown results (SD-1, SD-2, and SD-3) showed that when the mixers were off, ΔT significantly increased compared to ON-B1/ON-B2/ON-B3 and ON-A1/ON-A2/ON-A3 (SD-1: $H = 31.4$, $p < 0.001$, df = 2; SD-2: $H = 62.2$, $p < 0.001$, df = 2; SD-3: $H = 264.7$, $p < 0.001$, df = 2; Figure 5). During both ON-B1 and ON-A1, ΔT was significantly lower than ΔT at L2 and L3 (ON-B1: $H = 47.4$, $p < 0.002$, df = 2; ON-A1: $H = 119.1$, $p < 0.002$, df = 2; Figure 5). Similarly, ΔT during ON-B3 was significantly lower than ΔT at L2 and L3 (ON-B3: $H = 241$, $p < 0.001$, df = 2), suggesting that mixer operation only locally reduced temperature
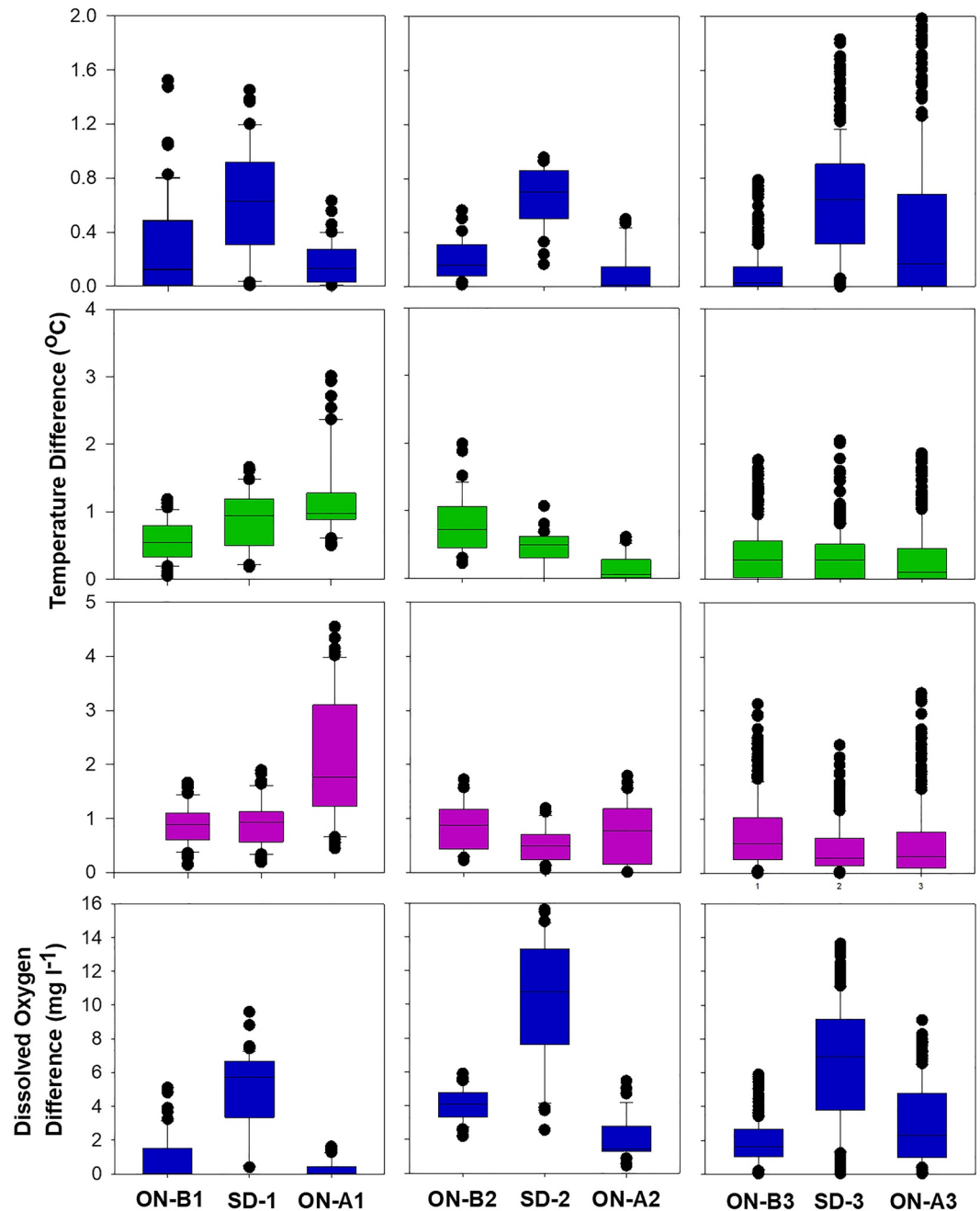
Figure 5. Box plots of temperature differences from B1 (blue), L2 (green), and L3 (purple) and dissolved oxygen difference at B1 during each shutdown (SD-1/SD-2/SD-3). Median line is shown on the box plots with the whiskers showing the 10th and 90th percentile. The differences from the ON periods, either side of each shutdown, are also shown.

gradients. Unlike at B1, ΔT did not consistently increase when the mixers were shut off at sites L2 and L3 (Figure 5), and meteorological conditions appeared to drive changes in ΔT.

3.3. Dissolved Oxygen

Mixer operation generally decreased the DO difference (ΔDO) between the hourly average surface and bottom water DO at site B1 (Figure 4d). During SD-1, air temperatures were significantly lower ($H = 140.8$; $p < 0.001$, df = 2; Figure 3a) and wind speeds were significantly higher ($H = 250$; $p < 0.001$, df = 2; Figure 3c), leading to
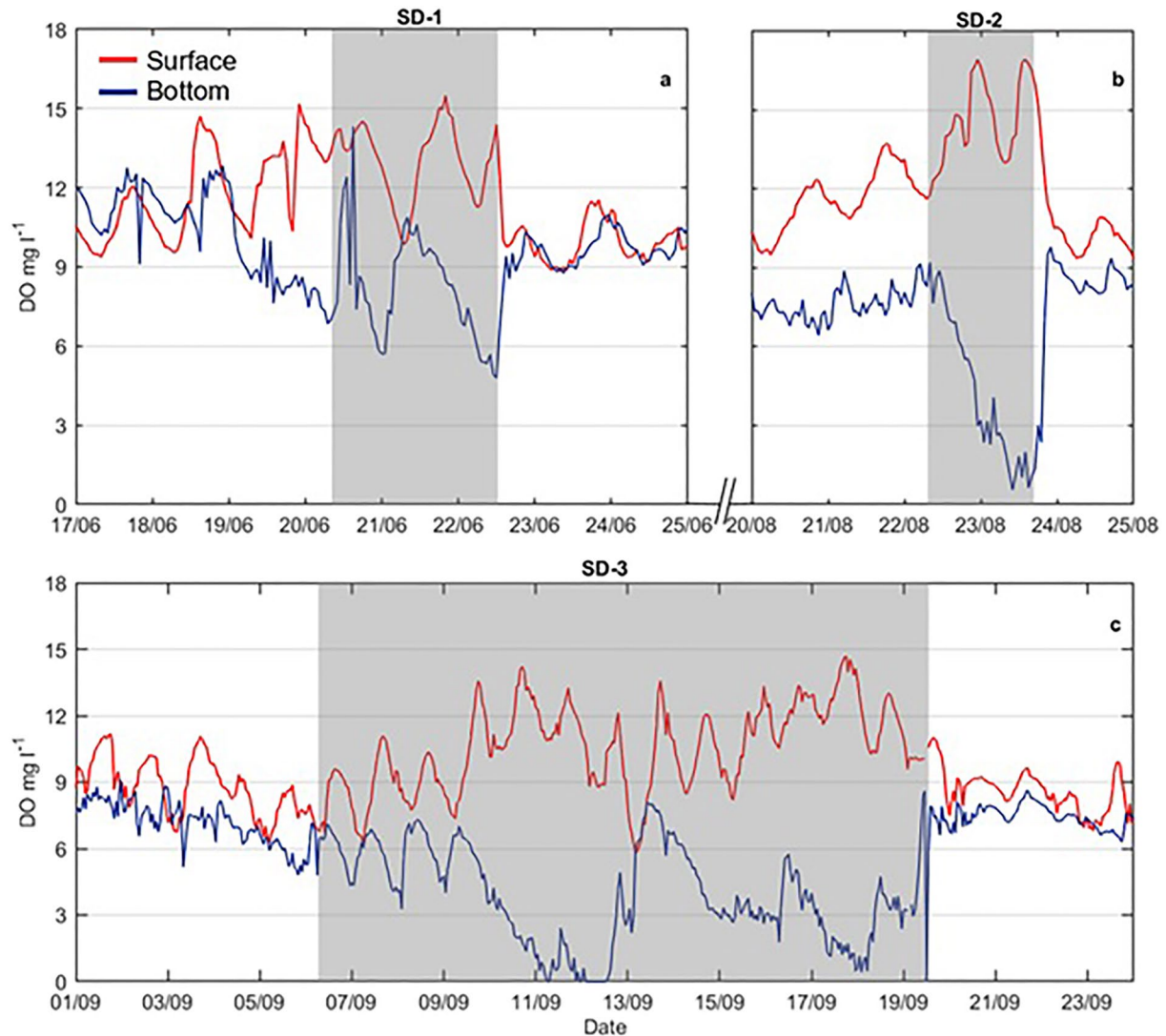
Figure 6. Hourly average dissolved oxygen at the surface (red line) and bottom (blue line) from B1 at Durleigh Reservoir for (a) SD-1, (b) SD-2, and (c) SD-3.

one natural mixing event in the middle of SD-1, where there was a peak in the combined TKE_{wind} and TKE_{conv} (Figure 3e). Nevertheless, ΔDO significantly increased during SD-1 compared to ON-B1 and ON-A1 ($H = 74.9$; $p < 0.001$, df = 2; Figure 5), indicating that mixer operation decreases ΔDO. When the mixers were turned back on (ON-A1), surface and bottom DO converge after 2 hr.

During SD-2, ΔDO significantly increased ($H = 71.9$; $p < 0.001$, df = 2; Figure 5) along with ΔT, suggesting that without mixer operation, large ΔDO may develop within 4 hr due to development of stratification. Almost immediately after the mixers were turned back on (ON-A2), the bottom and surface DO began to converge and the oxygen became well mixed after 3 hr (Figure 6). ΔDO remained small for the duration of ON-A2, which further indicates that the surface mixers influence DO distribution through the water column at B1. During ON-B2, ΔDO at B1 was high, corresponding with high DO at the surface (peaking at 170% saturation at 13:30 on August 21, 2018) caused by high phytoplankton productivity near the surface, whereas during ON-A2, ΔDO was significantly lower (DO at the surface reduced from 191% saturation at 14:00 on August 23 to 106% saturation at 03:30 on August 24, 2018) and likely caused by a combination of significantly higher wind speeds ($H = 80.8$; $p < 0.001$, df = 2; Figure 3c), lower air temperatures ($H = 378.1$; $p < 0.001$, df = 2; Figure 3a), and mixer operation. Nevertheless, mixer operation markedly decreased ΔDO over 6 m depth and 20 m from the mixers.

Prior to SD-3, ΔDO showed diurnal variations but averaged 1.8 mg l^{-1} for ON-B3 (Figure 5). The diurnal variation in ΔDO became more pronounced at the beginning of SD-3 before ΔDO increased on September 9, 2018 (Figure 4d). ΔDO during SD-3 was significantly higher than ΔDO during ON-B3 and ON-A3 ($H = 270.2$, $p < 0.001$, df = 2), despite a convergence on September 13, 2018 (Figure 4d). After the mixers were turned back on (ON-A3), ΔDO converged within 9 hr, which further demonstrates that the mixers are effective at quickly reducing DO gradients locally through the water column (Figure 6).

When occurring, the average oxygen flux into the lake due to wind was 0.6 g m^{-2} d^{-1} and the average flux due to convection was 0.9 g m^{-2} d^{-1}. There was no oxygen flux into the lake from the atmosphere during SD-1 and SD-2 as the surface was supersaturated with oxygen due to high algal productivity during daylight hours. During SD-3, the DO flux from convection reached 2 g m^{-2} d^{-1} at the same time that ΔDO dropped to 0 (Figures 4d and 4e).

3.4. Light Penetration

Measured Z_{SD} was in the range 0.2–0.7 m with minimal spatial variation observed, indicating that turbidity was high throughout the reservoir. With these low values, gradients between sites were likely masked by the accuracy of the measurements themselves, so it cannot be concluded whether light penetration at Durleigh was affected by mixer operation. Nevertheless, light penetration was low and based on these observations, the estimated euphotic depth ranged between 0.5 and 1.75 m. Similarly, 2015 SCAMP PAR sensor data used to estimate Z_{eu} showed an average of 1.55 ± 0.1 m (standard deviation) and a range of 1.44–1.72 m. Taking an average across all the estimates used for Z_{eu} gave 1.15 ± 0.28 m as the average euphotic depth.

3.5. Phytoplankton Distribution

Planktothrix agardhii, Dolichospermum flos-aquae, and *Aphanizomenon flos-aquae* were the dominant cyanobacteria species in the reservoir. *P. agardhii* were present in all water samples and counts were typically highest at L1 at all depths compared to L2 and L3. Counts of *P. agardhii* were significantly higher at L1S compared to L3S ($H = 4.38$; df = 2; $p = 0.02$); although counts at L1S were higher than L2S, the difference was not significant ($p = 0.09$). No other cyanobacteria showed statistically significant differences between locations.

In August, counts of *D. flos-aquae* were higher than counts of *P. agardhii* throughout Durleigh (see Text S5 and Figure S3 in Supporting Information S1). Counts of *D. flos-aquae* before and during SD-2 were generally higher at L1S compared to L1B (Figure S3 in Supporting Information S1) but the sample taken during ON-A2 showed higher counts of *D. flos-aquae* at L1B after the mixers were turned back on. Counts of *A. flos-aquae* were generally higher at the surface of L2 and L3 compared to L1S through August, indicating that water column stability may have benefited more buoyant cyanobacteria. However, due to the paucity of water samples collected during SD-2, we were unable to conclusively determine that mixer operation affected the vertical distribution of cyanobacterial cells through the water column.

While some variability was observed between counts at different depths at each site, these differences were not found to be statistically significant, so counts were depth averaged. Depth-averaged cyanobacteria counts (Figure 7a) were highest in August, which appears to be linked to an increase in counts of *D. flos-aquae* and *A. flos-aquae* (Figure S3 and Text S5 in Supporting Information S1); however, no significant differences were observed in the depth-averaged cyanobacterial counts between locations ($F_{(2,32)} = 0.95$; L1 and L2 $p = 0.63$; L1 and L3 $p = 0.38$; L2 and L3 $p = 0.95$). Depth averaged cell counts of *P. agardhii* (Figure 7b) were significantly higher at L1 compared to L2 and L3 ($F_{(2,32)} = 6.06$; L1 and L2 $p = 0.02$; L1 and L3 $p = 0.01$; L2 and L3 $p = 0.95$). No significant differences were found between depth-averaged counts of *D. flos-aquae* or *A. flos-aquae*.

4. Discussion

Surface mixers are increasingly being used by industry to mitigate against deterioration of raw water quality in drinking water supply reservoirs, but there is limited evidence that mixers successfully optimize water quality, particularly for shallow reservoirs. With this novel study, we have obtained in-situ observations of how artificial circulation induced by surface mixers affects hydrodynamics, temperatures, DO concentration, turbidity and related sediment resuspension, and cyanobacterial cell distributions. Results indicate that the principal reservoir management goals of maintaining destratification and homogeneous temperature and DO distributions were only
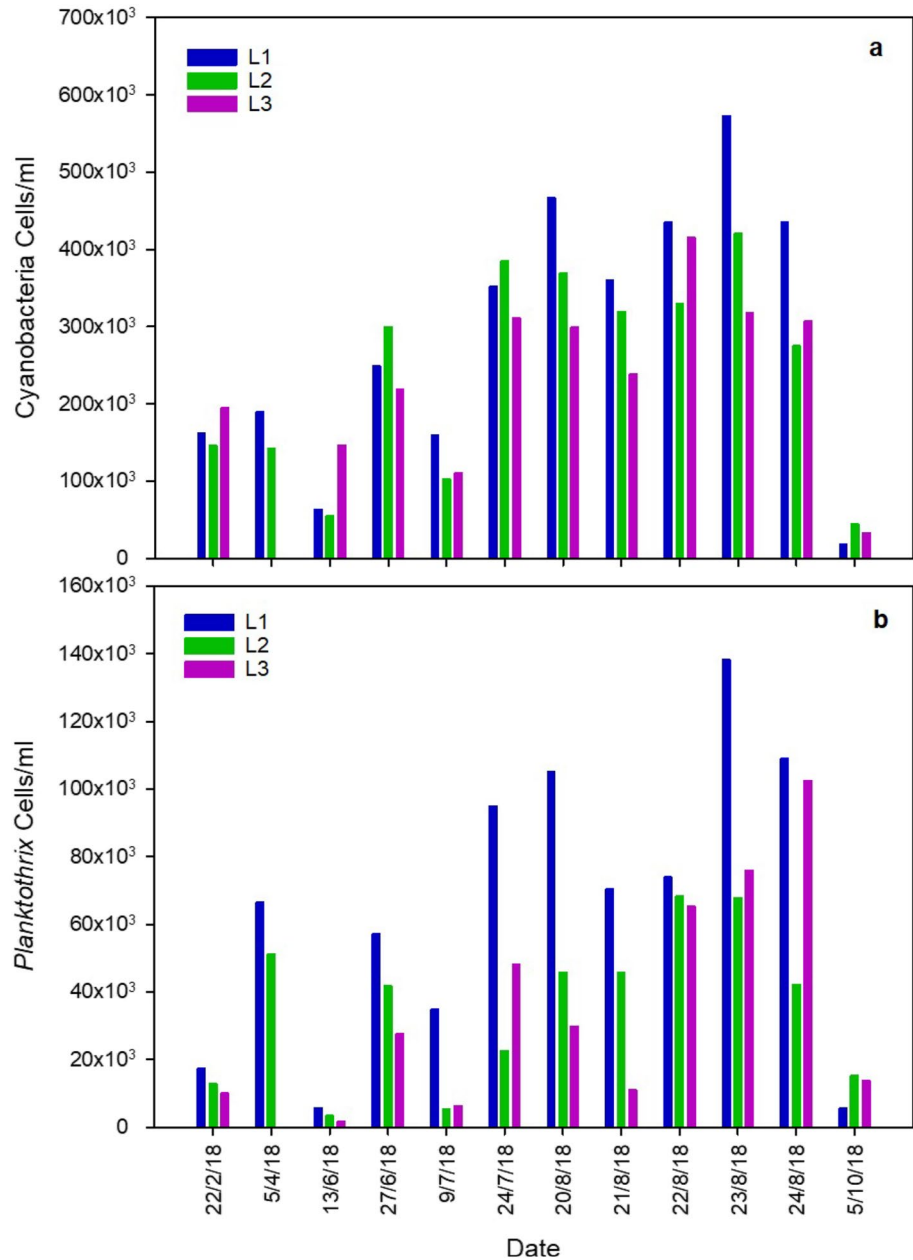
Figure 7. (a) Depth averaged cyanobacteria cell counts at L1, L2, and L3 in Durleigh Reservoir over 2018. (b) Depth averaged *Planktothrix agardhii* cell counts at L1, L2, and L3. The surface mixer was not operating on August 22 and 23, 2018.

achieved within a local area around the mixers, beyond which influence of the mixers is not obviously discernible from meteorological effects. Implications for water quality and surface mixer operations are discussed below.

4.1. Temperature

Artificial circulation using surface mixers seeks to prevent thermal stratification from forming. Although L2 is only ~0.5 m shallower than B1, RTRM exceeds values of 30 and 80 more frequently, which suggests that the effects of the mixers are reduced at a distance of 60 m. During all shutdowns, ΔT at B1 increased significantly (Figure 5) and was attributed to the mixers being turned off, whereas changes in ΔT at L2 or L3 appear to be influenced more by meteorological conditions. Similarly, Upadhyay et al. (2013) reported very localized

effects of a solar-powered upward mixer on ΔT (5–10 m radius) and values of calculated cumulative relative thermal resistance to mixing (3 m radius). Temperature profiles at Myponga reservoir (36 m maximum depth) showed weakened stratification 300 m from a top-down surface mixer (4.9 m diameter) with a draft tube (Lewis et al., 2010). Han et al. (2020) reported that the use of a solar-powered upward mixer in the shallow and turbid Jordan Lake had minimal impact when compared to meteorological mixing inputs.

At B1, bottom water temperatures were significantly higher than L2 and L3, suggesting that mixer operation locally circulates warmer surface waters downwards. Warmer temperatures in the hypolimnion strongly affect biogeochemical processes at the sediment-water interface (SWI; Bell & Ahlgren, 1987). For example, warmer temperatures at the SWI can increase rates of mineralization of organic matter and lead to increased microbial respiration, which increase DO demand. Jiang et al. (2008) found that bacterial respiration at the SWI increased with warmer temperatures, which lowered the redox potential and resulted in a release of iron and manganese from the sediments to the overlying water, with consequent release of iron-bound phosphate. Overall, top-down surface mixers locally decrease ΔT (<20 m distance) via increasing bottom water temperatures.

4.2. Dissolved Oxygen

Theoretically, surface mixer operation moves oxygenated surface waters down through the water column to the hypolimnion and sediments, where DO demand is typically highest (Beutel & Horne, 1999). Elevated DO concentrations were observed at the surface of B1 during all shutdowns (Figure 6), but highest during SD-2 in August, when air temperatures were high and when the highest cyanobacterial cell counts were observed (Figure 7a). A diurnal cycle of DO was observed at the surface in August, reflecting photosynthesis during the day and respiration overnight. Despite increased respiration overnight, the DO largely remained elevated. Positively buoyant cyanobacteria such as *Aphanizomenon* and *Dolichospermum* may have capitalized on the reduced mixing to remain in the photic zone for longer (Visser et al., 2016). Therefore, turning off the mixers likely increased surface DO at B1 indirectly through reduced transport of phytoplankton cells out of the photic zone. The surface waters were supersaturated with oxygen during SD-1 and SD-2, preventing reaeration from the atmosphere.

Oxygen deficits near the sediments are associated with increased BOD during the mineralization of phytoplankton biomass after death and sedimentation (Wetzel, 1983). During all shutdowns, DO near the bottom of the water column declined (Figure 6), which is likely due to the mixer shutdown decreasing transport of DO downwards from the surface waters. For each post-shutdown period, the time taken for the ΔDO to decrease was relatively fast, declining to <2 mg l^{-1} ΔDO within less than 2, 5, and 8 hr for SD-1, SD-2, and SD-3, respectively, corresponding to oxygen consumption rates of 5, 6, and 3 g m^{-3} d^{-1}. Because the surface layer was supersaturated, this indicates that vertical mixing was the constraining factor in reoxygenation of the bottom waters and the rapid decline in ΔDO following the restarting of the mixers was most likely a result of their operation.

4.3. Flow Velocities, Transport, and Sediment Resuspension

High flow velocities generated by surface mixers can lead to localized circulation cells forming around the mixers; however, if flow velocities are too low, the desired effects of mixing will not be achieved (Punnett, 1991). For example, Lawson and Anderson (2007) observed vertical velocities of 0.3 m s^{-1} adjacent to the top-down mixers (although 0.72 m s^{-1} is the assumed initial flow velocity) in Lake Elsinore; these high velocities were acknowledged as the cause of localized circulation cells with a 24 m radius around the pumps. These circulation cells are hypothesized to be the result of the pumping flow rate exceeding the flow rate at which mixed water moves away into the lake interior, with the idea that the flow structure in Figure 1b is more efficient at mixing the lake over a broader extent than Figure 1a (Punnett, 1991).

By examining some of the properties of the turbulence near the mixers, the potential for intrusion generation (as in Figure 1b) can be determined. Following Lemckert and Imberger (1995) who examined axisymmetric intrusion formation from a bubble plume in a stratified reservoir (which causes mixing from the bottom as opposed to the surface as in this scenario), the turbulent Froude number ($Fr_T = \varepsilon / NL_C^{2/3}$), turbulent Reynolds number ($Re_T = \varepsilon^{1/3} L_C^{4/3} / v$), and turbulent Grashof number ($Gr_T = NL_C^2 / v$) were calculated, where $\varepsilon = 2.2 \times 10^{-7}$ W kg^{-1} (Text S1 in Supporting Information S1), $N = 0.012$ s^{-1} is the average background buoyancy frequency measured at L2, and $L_C = 0.16$ m is the centered displacement scale, here approximated by the Thorpe scale from the SCAMP measurements at S1 using the method of Ferron et al. (1998). For one mixer, Fr$_T$ = 1.7, Re$_T$ = 520,

and $Gr_T = 310$, indicating that the turbulence near the mixers is best described by an inertia-buoyancy balance. Lemckert and Imberger ([1993](#)) estimated the distance at which an axisymmetric intrusion governed by an inertia-buoyancy balance will travel before viscosity effects begin as $L = 0.91 \left(Q^3 / N \nu^2 \right)^{1/5}$ where Q is the flow rate in the intrusion. While Q is nominally 0.67 m^3 s^{-1} from the mixer, this flow rate gives a distance L of over 400 m, which is not observed in the data, The maximum intrusion distance in Durleigh is less than 60 m; solving for Q then gives an intrusion flow rate of 0.028 m^3 s^{-1}, approximately 4% of the flow from the mixers.

Measurements of the flow field around mixers are crucial for understanding the radius of influence, but only few such measurements exist. Horizontal velocities were in the range 0.1–0.2 m s^{-1} up to 20 m from the mixers in Lake Elsinore, and ∼0.02 m s^{-1} beyond 20 m. Comparably, each mixer at Durleigh has an initial flow velocity of 0.15 m s^{-1}, which is only half that of the observed mixer velocities in Lake Elsinore and the velocity magnitude near the sediment surface at Durleigh was generally below 0.05 m s^{-1} (Figure S2b in Supporting Information [S1](#)). Nevertheless, the high-resolution, single-point ADV data indicated that mixers influence near-bed flow velocities up to ∼30 m away.

ADV amplitude data from Durleigh (Figure S2c in Supporting Information [S1](#)) showed that the concentration of suspended particles in the water column decreased significantly during SD-2, which suggests that the mixers may be responsible for increasing sediment resuspension. The mixer plume was expected to impinge upon the bottom over 75% of the measurement period. Sediment resuspension is problematic for water quality due to increased turbidity and potential release of metals and nutrients from the sediment porewater into the water column (Matisoff et al., [2017](#); You et al., [2007](#)). Therefore, it is likely that the localized sediment resuspension around the mixers at Durleigh increased the availability of nutrients in the water column. The depth of the water column varies significantly over a season in drinking water reservoirs due to abstraction, inflows, and evaporation, with shallower water levels further increasing the risk of sediment resuspension (Effler & Matthews, [2007](#)). The decrease in amplitude during SD-2 occurred overnight (Figure S2c in Supporting Information [S1](#)), coinciding with a drop in wind speeds. Bioturbation from the benthic feeding fish at Durleigh may have contributed to resuspension (Barton et al., [2000](#)), although this is unlikely as bioturbation is sporadic and would not reflect an obvious decrease when the mixers were turned off during SD-2. The decline in suspended particles during SD-2 was likely due to a combination of the mixers being turned off and reduced meteorological forcing. To reduce localized sediment resuspension when the mixers are operating, options such as installing a deflection plate, reducing mixer flow rate, or varying the mixer flow rate as a function of water column depth should be investigated as part of mixer installation best practice for shallow reservoirs.

4.4. TKE Inputs

Field observations showed that the mixers were effective over a radius of 30 m but their effects over 60 m were not obviously discernible from meteorological effects. Therefore, we suggest that the area of influence of the mixers was likely to cover an area between 2,800 and 11,300 m^2 (30–60 m radius). When Durleigh is at full capacity, the area of influence ranges between 1% and 3% of the total surface area or the reservoir. During SD-2, when the depth of the water column was 2 m below full capacity, the area of influence of the mixers was in the range 3%–14%. Consequently, when the water depth in the reservoir decreases, the mixers influence a greater percentage of the total surface area.

The TKE$_{mix}$ input of one mixer per unit area at Durleigh is 1.7 W m^{-2}, compared to 195 W m^{-2} for one top-down pump from Lake Elsinore (Lawson & Anderson, [2007](#)), calculated using Equation [4](#). Therefore, the TKE$_{mix}$ input of each pump at Lake Elsinore is over 100 times than the TKE$_{mix}$ input of one mixer at Durleigh, and despite the greater inputs of energy from the pumps in Lake Elsinore, mixing was still found to be limited. Distributing the TKE input from mixers over the range of influence from the field observations (30–60 m), yields an average TKE between 2.1 and 8.1 × 10^{-3} W m^{-2} with three mixers on (conditions until SD-1), 1.4–5.4 × 10^{-3} W m^{-2} with two mixers on (conditions after SD-1), and 0.7–2.7 × 10^{-3} W m^{-2} with one mixer on (2015 conditions). Generally, TKE$_{mix}$ over the maximum estimated area of influence (60 m radius) was greater than the combined energy inputs from TKE$_{wind}$ and TKE$_{conv}$ (Figure [3e](#)) indicating that the continuous TKE input from the mixers is greater than natural inputs over the localized area of influence.

Read et al. (2012) examined the relative influence of wind and convection in driving mixing over 40 lakes. The average ratio between u_* and w_* in Durleigh was 0.55, indicative of a lake where convection dominates over wind mixing, which falls in line with lakes of similar surface area from that work. But while the average TKE input from convection was higher than that from wind, wind events generated the highest TKE inputs from natural sources throughout the study period, particularly when hourly averaged wind speeds were >7 m s^{-1} due to increased wave heights and resulting in increased drag coefficient (Wüest & Lorke, 2003).

The net heat flux is comprised of the net shortwave radiation, net longwave radiation, sensible heat flux, and latent heat flux. The relative importance of each of these terms depends upon local climate. For instance, the magnitude of these fluxes observed for Durleigh is similar to those observed by Woolway et al. (2015) for Lake Mendota (WI, USA) and Esthwaite Water (UK) which are in cooler wetter climates but were smaller than those estimated by Saber et al. (2018) in summer for Lake Mead (NV/AZ, USA) where local climate is hot and dry. But for both Lake Mead and this data set, the largest TKE input from convection occurred during periods of high latent heat flux, for example, the mixing event during SD-1 appeared to be driven by cold dry air. By comparison, the large air temperature drop during SD-3 was associated with increased relative humidity, thus resulting in a less significant increase in latent heat flux. While LHFA uses common approximations to estimate the incoming and outgoing longwave radiation, the lack of direct measurements leads to uncertainty in the role of these in the heat budget. The uncertainty analysis indicates that the TKE from convection might vary by a factor of 2 from the estimated values, but values still remain below that of the low estimate for the mixers (Figure 3d).

4.5. Light Penetration, Mixing, and Cyanobacteria Distribution

Shallow eutrophic reservoirs are typically more turbid, which favor shallower diurnal temperature stratification, but stratification frequency and regularity depend on meteorological conditions (Stepanenko et al., 2013). At Durleigh, turbidity was high and the estimated euphotic depth was shallow, typically less than 1.55 m. Due to the observed sediment resuspension around the mixers, nutrients were not considered to be a limiting factor for phytoplankton growth. Low light, turbid, and polymictic conditions are reported to benefit *Planktothrix* over other genus' by homogenously distributing filaments through the water column and maintaining light-limited conditions (Ibelings et al., 2021). At Durleigh, consistently higher counts of *P. agardhii* were observed at L1, closest to the mixers compared to L2 and L3. Counts of *D. flos-aquae,* were high in water samples collected from all locations and depths in August and counts of *A. flos-aquae* were higher at the surface of L2 and L3 compared to L1. The use of cell counts over biovolume estimates limits the interpretation of the phytoplankton data presented here as differences in relative sizes of the species identified are not considered. For example, the Biovolume Calculator from the Victoria State Government (2015) considers the mean cell volume of *D. flos aquae* to be 56 μm^3 and *P. agardhii* to be 47 μm^3, which would give different biovolumes for the equivalent cell count values. Cell count data is more applicable for comparison of existing data held by water utilities in England and Wales, but highlights that water managers should perhaps consider biovolumes to better understand the phytoplankton composition in raw water sources.

During July and August, the TN:TP ratio at Durleigh was low due largely to a decrease in nitrate concentrations (Slavin, 2021). A low TN:TP ratio has been associated with increases in *A. flos-aquae* (Cottingham et al., 2015), a species that also has buoyancy regulating mechanisms (Reynolds et al., 1987). RTRM at L2 and L3 showed a diurnal pattern increasing during the day and decreasing at night, reflective of diurnal stratification. Diurnal stratification outside the range of influence of the mixers most likely developed because of low light penetration heating the uppermost layers of the water column and convective cooling at night. Infrequent wind mixing events may be sufficient to mix the water column away from the mixers but generally, outside the range of influence of the mixers, diurnal stratification conditions may benefit buoyant cyanobacteria.

In light-limited water bodies with diurnal stratification such as Durleigh, vertical mixing plays a key role in regulating the distribution of DO, nutrients, and phytoplankton. Artificial mixing is meant to (a) prevent stratification and ensure oxygen penetration to the bottom waters, preventing release of soluble forms of iron, phosphorus, and manganese from the sediments, and (b) reduce the competitive advantage of buoyancy-regulating cyanobacteria by creating enough mixing to overwhelm the floating velocities of buoyant cyanobacteria. As discussed in 4.1 and 4.2, the mixers succeeded in the first objective near the mixers at B1, but this effect was local. The higher counts of *P. agardhii* at L1 throughout 2018 indicate that the localized effects of surface mixers may increase nutrient availability from sediment resuspension, which benefits growth We therefore propose that the operation

of surface mixers in shallow eutrophic reservoirs benefits low-light adapted filamentous cyanobacteria species, such as *P. agardhii* and suggest that surface mixers are unlikely to provide successful cyanobacteria control under these conditions.

Values of eddy diffusivity have been used in the competition model proposed by Huisman et al. (2004) to determine how changes in turbulent mixing induced by bubble curtains change competition for light between buoyant and non-buoyant phytoplankton. Huisman et al. (2004) reported $K = 1.7 \times 10^{-5}$ m^2 s^{-1} without artificial mixing and 5.1×10^{-4} m^2 s^{-1} with artificial mixing. In addition, Huisman et al. (2004) demonstrated that a significant increase in turbulent diffusivity caused by artificial mixing with air curtains resulted in a shift away from a *Microcystis*-dominated assemblage to a greens/diatoms-dominated phytoplankton community.

The eddy diffusivity observed in 2015 near the mixers ($K = 4.4 \times 10^{-5}$ m^2 s^{-1}) was similar to that observed by SCAMP measurements near an updraft mixer, where water is drawn up from the bottom (Han et al., 2020). Although the values of K observed near the mixers were lower than that due to bubblers in Huisman et al. (2004), Péclet number considerations indicated that the mixing was sufficient to move some cells through the water column. The Péclet number ($Pe = \tau_{mix}/\tau_w = (w * H)/K$) is a ratio between the time scales of turbulent mixing ($\tau_{mix} = H^2/K$) and vertical velocity ($\tau_w = H/w$; sinking/floating), where w is the vertical velocity of the cell and H is the water depth. $Pe > 1$ indicates that vertical flotation velocities exceed the rate of turbulent mixing, whereas $Pe < 1$ indicates turbulent mixing dominates over vertical velocity and homogenous mixing is more likely (Visser et al., 2016). For *Planktothrix*, Pe calculated at L1 ($H = 5$ m depth; $K = 4.4 \times 10^{-5}$ m^2 s^{-1}) using $w = 6.21$ µm s^{-1} (Walsby & Holland, 2006) is 0.7, demonstrating that turbulent mixing likely dominates over vertical velocities of phytoplankton. Using the maximum floating velocities for *A. flos-aquae* (7 µm s^{-1}) and *D. flos-aquae* (10 µm s^{-1}) reported by Reynolds et al. (1987), Pe calculated at L1 is 0.8 and 1.1, respectively. Therefore, the observed values of K at L1 when only one mixer is operating, may not be enough to overwhelm the vertical floating velocities of *D. flos-aquae*. During the August 2018 experiment, *D. flos-aquae* counts were higher at the surface than the bottom at L1 before the mixers were shut off and remained so during SD-2 (Figure S3 in Supporting Information S1). Turning the mixers on following SD-2 appeared to decrease *D. flos-aquae* counts at the surface of L1 and increased counts at the bottom of the water column (Figure S3 in Supporting Information S1), possibly indicating that operation of the mixers was sometimes (but not always) enough to successfully overwhelm the floating velocities of *D. flos-aquae*. We hypothesize that the turbulent diffusivities from the mixers may not be sufficient to overwhelm the vertical velocities of more buoyant species such as *D. flos-aquae* but further research is required to confirm this hypothesis.

While Huisman et al. (2004) observed a shift from cyanobacteria to green algae and diatoms, a similar effect was not observed at light-limited Durleigh. At 20 m from the mixers, mixer operation appeared to benefit *P. agardhii* throughout the study period, which may have been caused by localized sediment resuspension leading to increased nutrient availability. The vertical velocities of *Planktothrix* may be overwhelmed by turbulent mixing from within the range of influence of the mixers but it is not clear whether we are observing redistribution of cells through the water column at L1. However, we observed higher cell counts of *Planktothrix* at L1 through 2018 compared to L2 and L3, indicating there may be a benefit to *Planktothrix* growth and not just redistribution of filaments through the water column. The maximum specific growth for *Planktothrix* spp. in culture studies was reported to range between 0.12 and 1.15 days^{-1} (Halstvedt et al., 2007). A coarse estimate of turnover time within the range of influence of the mixers indicates that when two mixers are operating at their maximum flow rate, the volume of water within a 30 and 60 m radius of the mixers (6.5 m depth) turns over every 3.8 and 15.2 hr, respectively. Mixer operation is likely controlling cell distributions through the water column within the range of influence of the mixers, but cells may be accessing light and nutrients required for growth every few hours, which may impact upon growth processes. Further research into the impacts of localized mixing on *Planktothrix* growth rates is needed to confirm whether mixing has any effect on phytoplankton succession.

Nonetheless, operation of the mixers likely provides *P. agardhii* with a competitive advantage over other cyanobacteria by passively transporting filaments to nutrients made available through localized sediment resuspension and maintaining low light conditions. Rücker et al. (1997) found *P. agardhii* tended to dominate in shallow eutrophic lakes that stratified less frequently. Chorus and Welker (2021) suggested that *P. agardhii* may prevent other cyanobacteria from growing by maintaining the system in turbid and light limited conditions, which could be what we see exacerbated by the mixers at Durleigh, distributing the cells through the water column. Although

spacing the mixers out to cover a greater surface area of the lake may improve the reaeration of bottom waters over a greater extent, it is unlikely to control cyanobacteria.

5. Conclusions

The top-down surface mixers appeared to influence a highly localized area (30–60 m radius; 1%–3% total surface area at full capacity), but artificial circulation over the localized area was shown to be effective at significantly reducing water column temperature and oxygen gradients. The mixers were the dominant driver of reaeration of bottom waters within this area. Energy input from the mixers over the region of influence exceeded energy inputs from wind and convection by over an order of magnitude. Localized sediment resuspension was observed because of mixer operation, which could exacerbate the release of soluble metals and nutrients from the sediments. Away from the mixers, diurnal stratification was observed due to a combination of solar radiation, turbidity, and low light penetration that prevented the transfer of heat through the water column at times when meteorological forcing was insufficient to mix the water column. Consequently, the impacts of stratification on water quality are likely to still occur outside of the area of influence of the mixers.

Based on the observations at Durleigh, we hypothesize that within the range of influence of the top-down mixers, passively transported cyanobacteria cells and filaments have cyclical access to nutrients resuspended from the sediments, which may benefit cyanobacteria growth processes. During periods of warming, we propose that turbulent diffusivities from surface mixers may not be sufficient to overwhelm the vertical velocities of more buoyant cyanobacteria, although further research is required to confirm this hypothesis. Overall, top-down surface mixers are unlikely to effectively control cyanobacteria in shallow, turbid reservoirs.

Data Availability Statement

Data presented in this study are freely available: *ADV Data*: https://doi.org/10.5285/fd3eb9f3-832e-4a16-b9db-fd6045242ecf; *Light*: https://doi.org/10.5285/fc1cf9a7-d7b0-4948-8328-497d6e071950; *DO*: https://doi.org/10.5285/26b35c45-c174-4930-b82c-bcd0d23c39e1. Weather: https://doi.org/10.5285/dcfa74ce-6d05-4717-978d-e7cdf9b2039e; *Water Chemistry*: https://doi.org/10.5285/f5f85f15-8f3a-474c-ae58-7cdeab2a53ca; *Water Temperature*: https://doi.org/10.5285/25d34c83-e939-40fd-aa16-6962efb4c731.

References

Barton, D. R., Kelton, N., & Edey, R. I. (2000). The effects of carp (*Cyprinus carpio* L.) on sediment export from a small urban impoundment. *Journal of Aquatic Ecosystem Stress and Recovery*, *8*, 155–159. https://doi.org/10.1023/A:1011423432727

Bell, R. T., & Ahlgren, I. (1987). Thymidine incorporation and microbial respiration in the surface sediment of a hypereutrophic lake. *Limnology & Oceanography*, *32*, 476–482. https://doi.org/10.4319/lo.1987.32.2.0476

Beutel, M. W., & Horne, A. J. (1999). A review of the effects of hypolimnetic oxygenation on lake and reservoir water quality. *Journal of Lake and Reservoir Management*, *15*, 285–297. https://doi.org/10.1080/07438149909354124

Chanson, H., Takeuchi, M., & Trevethan, M. (2008). Using turbidity and acoustic backscatter intensity as surrogate measures of suspended sediment concentration in a small subtropical estuary. *Journal of Environmental Management*, *88*, 1406–1416. https://doi.org/10.1016/j.jenvman.2007.07.009

Chorus, I., & Welker, M. (2021). *Toxic cyanobacteria in water: A guide to their public health conseqeuences, monitoring and management* (2nd ed.). Oxon:CRC Press (ISBN: 978-1-003-08144-9).

Chung, E. G., Bombardelli, F. A., & Schladow, S. G. (2009). Modelling linkages between sediment resuspension and water quality in a shallow, eutrophic, wind-exposed lake. *Ecologcial Modelling*, *220*, 1251–1265. https://doi.org/10.1016/j.ecolmodel.2009.01.038

Cottingham, K. L., Ewing, H. A., Greer, M. L., Carey, C. C., & Weathers, K. C. (2015). Cyanobacteria as biological drivers of lake nitrogen and phosphorus cycling. *Ecosphere*, *6*(1), 1–19. https://doi.org/10.1890/es14-00174.1

Delta T Devices Ltd. (2016). *WS-GP1 weather station [Online]*. Microsoft Word - WS_GP1_Data_Sheet_version_2.docx (delta-t.co.uk)

Dokulil, M. T., & Teubner, K. (2003). Steady state phytoplankton assemblages during thermal stratification in deep alpine lakes. Do they occur? *Hydrobiologia*, *502*, 65–72. https://doi.org/10.1023/B:HYDR.0000004270.70364.f3

Effler, S. W., & Matthews, D. A. (2007). Sediment resuspension and drawdown in a water supply reservoir. *Journal of the American Water Resources Association*, *40*, 251–264. https://doi.org/10.1111/j.1752-1688.2004.tb01023.x

Elliott, S., & Swan, D. (2013). Source water management – Deep reservoir circulation. *Paper presented at 7th annual WIOA NSW water industry operations conference. Exhibition park in Canberra* (pp. 84–91). Retrieved from http://www.wioa.org.au/conference_papers/2013_nsw/documents/Stephen_Elliott.pdf

Ferron, B., Mercier, H., Speer, K., Gargett, A., & Polzin, K. (1998). Mixing in the Romanche Fracture Zone. *Journal of Physical Oceanography*, *28*, 1929–1945. https://doi.org/10.1175/1520-0485(1998)028<1929:mitrfz>2.0.co;2

Gray, E., Mackay, E., Elliott, A., Folkard, A. M., & Jones, I. (2020). Wide-spread inconsistency in estimation of lake mixed depth impacts interpretation of limnological processes. *Water Research*, *168*, 115–136. https://doi.org/10.1016/j.watres.2019.115136

Ha, H. K., Hsu, W.-Y., Maa, J. P.-Y., Shao, Y. Y., & Holland, C. W. (2009). Using ADV backscatter strength for measuring suspended cohesive sediment concentration. *Continental Shelf Research*, *29*, 1310–1316. https://doi.org/10.1016/j.csr.2009.03.001

Halstvedt, C. B., Rohrlack, T., Andersen, T., Skulberg, O., & Edvardsen, B. (2007). Seasonal dynamics and depth distribution of *Planktothrix* spp. in Lake Steinsforden (Norway) related to environmental factors. *Journal of Plankton Research*, *29*, 471–482. https://doi.org/10.1093/plankt/fbm036

Hammer, O., Harper, D. A. T., & Ryan, P. D. (2001). PAST: Paleontological statistics software package for education and data analysis. https://palaeo-electronica.org/2001_1/past/past.pdf

Han, Y., Smithheart, J. W., Smyth, R. L., Aziz, T. N., & Obenour, D. R. (2020). Assessing vertical diffusion and cyanobacteria bloom potential in a shallow eutrophic reservoir. *Lake and Reservoir Management*, *36*, 169–185. https://doi.org/10.1080/10402381.2019.1697402

Harris, T. D., Wilhelm, F. M., Graham, J. L., & Loftin, K. A. (2014). Experimental manipulation of TN:TP ratios suppress cyanobacterial biovolume and microcystin concentration in large-scale in situ mesocosms. *Lake and Reservoir Management*, *30*, 72–83. https://doi.org/10.1080/10402381.2013.876131

Huisman, J., Sharples, J., Stroom, J. M., Visser, P. M., Kardinaal, W. E. A., Verspagen, J. M. H., & Sommeijer, B. (2004). Changes in turbulent mixing shift competition for light between phytoplankton species. *Ecology*, *85*, 2960–2970. https://doi.org/10.1890/03-0763

Ibelings, B. W., Kurmayer, R., Azevedo, S. M. F. O., Wood, S. A., Chorus, I., & Welker, M. (2021). Understanding the occurrence of cyanobacteria and cyanotoxins. In I. Chorus, & M. Welker (Eds.), *Toxic cyanobacteria in water: A guide to their public health consequences, monitoring and management* (2nd ed.). https://doi.org/10.1201/9781003081449

Imboden, D. M. (1980). The impact of pumped storage operation on the vertical temperature structure in a deep lake: A mathematical model. In J. P. Clugston (Ed.), *Proceedings of the Clemson workshop on environmental impacts of pumped storage hydroelectric operations* (Vol. 80/28, pp. 125–146). Fish and Wildlife Services, US Department of the Interior, FWS/OBS

Ismail, R., Kassim, M. A., Inman, M., Baharim, N. H., & Azman, S. (2002). Removal of iron and manganese by artificial destratification in a tropical climate (Upper Layang Reservoir, Malaysia). *Water Science and Technology*, *46*(9), 179–183. https://doi.org/10.2166/wst.2002.0234

Jiang, X., Jin, X., Yao, Y., Li, L., & Wu, F. (2008). Effects of biological activity, light, temperature and oxygen on phosphorus release processes at the sediment and water interface of Taihu Lake, China. *Water Research*, *42*, 2251–2259. https://doi.org/10.1016/j.watres.2007.12.003

Kerimoglu, O., & Rinke, K. (2013). Stratification dynamics in a shallow reservoir under different hydro-meteorological scenarios and operational strategies. *Water Resources Research*, *49*, 7518–7527. https://doi.org/10.1002/2013WR013520

Lawson, R., & Anderson, M. A. (2007). Stratification and mixing in Lake Elsinore, California: An assessment of axial flow pumps for improving water quality in a shallow eutrophic lake. *Water Research*, *41*, 4457–4467. https://doi.org/10.1016/j.watres.2007.06.004

Lemckert, C. J., & Imberger, J. (1993). Axisymmetrical intrusive gravity currents in linearly stratified fluids. *Journal of Hydraulic Engineering*, *119*(6), 662–679. https://doi.org/10.1061/(asce)0733-9429(1993)119:6(662)62)

Lemckert, C. J., & Imberger, J. (1995). Turbulence within inertia- buoyancy balanced axisymmetric intrusions. *Journal of Geophysical Research*, *100*(C11), 22649–22666. https://doi.org/10.1029/95JC00274

Lewis, D. M., Lambert, M. F., Burch, M. D., & Brookes, J. D. (2010). Field measurements of mean velocity characteristics of a large-diameter swirling jet. *Journal of Hydraulic Engineering*, *136*, 642–650. https://doi.org/10.1061/(ASCE)HY.1943-7900.0000207

Li, N., Huang, T., Mao, X., Zhang, H., Wen, G., Lv, X., et al. (2019). Controlling reduced iron and manganese in a drinking water reservoir by hypolimnetic aeration and artificial destratification. *Science of the Total Environment*, *685*, 497–507. https://doi.org/10.1016/j.scitotenv.2019.05.445

Lindenschmidt, K. E., & Chorus, I. (1998). The effect of water column mixing on phytoplankton succession, diversity and similarity. *Journal of Phytoplankton Research*, *20*, 1927–1951. https://doi.org/10.1093/plankt/20.10.1927

Luhtala, H., & Tolvanen, H. (2013). Optimizing the use of Secchi depth as a proxy for euphotic depth in coastal waters: An empirical study from the Baltic Sea. *ISPRS International Journal of Geo-Information*, *2*, 1153–1168. https://doi.org/10.3390/ijgi2041153

Lund, J. W., Kipling, G., & Le Cren, E. D. (1958). The inverted microscope method of estimating algae numbers and the statistical basis of estimation by counting. *Hydrobiologia*, *11*, 143–170. https://doi.org/10.1007/BF00007865

Mackay, E., Jones, I., Thackery, S., & Folkard, A. (2011). Spatial heterogeneity in a small, temperate lake during archetypal weak forcing conditions. *Fundamental and Applied Limnology*, *179*, 27–40. https://doi.org/10.2307/1467544

Matisoff, G., Watson, S. B., Guo, J., Duewiger, A., & Steely, R. (2017). Sediment and nutrient distribution and resuspension in Lake Winnipeg. *Science of the Total Environment*, *575*, 173–186. https://doi.org/10.1016/j.scitotenv.2016.09.227

Morillo, S., Imberger, J., Antenucci, J. P., & Copetti, D. (2009). Using impellers to distribute local nutrient loadings in a stratified lake: Lake Como, Italy. *Journal of Hydraulic Engineering*, *135*, 564–574. https://doi.org/10.1061/(ASCE)HY.1943-7900.0000048

Onset Computer (2018). Tidbit v2 temp (UTBI-001) manual. Retrieved from: https://www.onsetcomp.com/files/manual_pdfs/10385-J 0UTBI-001 0Manual.pdf

Osborn, T. R., & Cox, C. S. (1972). Oceanic fine structure. *Geophysical Fluid Dynamics*, *3*, 321–345. https://doi.org/10.1080/03091927208236085

Perkins, R. G., Slavin, E. I., Andrade, T. M. C., Blenkinsopp, C., Pearson, P., Froggatt, T., et al. (2019). Managing taste and odour metabolie production in drinking water reservoirs: The importance of ammonium as a key nutrient trigger. *Journal of Environmental Management*, *244*, 276–284. https://doi.org/10.1016/j.jenvman.2019.04.123

Punnett, R. E. (1991). *Design and operation of axial flow pumps for reservoir destratification*. U.S. Army Corps of Engineers.

RBR. (2021). RBRsolo T compact temperature logger. Retrieved from https://rbr-global.com/product-page-experiment

Read, J. S., Hamilton, D. P., Desai, A. R., Rose, K. C., MacIntyre, S., Lenters, J. D., et al. (2012). Lake-size dependency of wind shear and convection as controls on gas exchange. *Geophysical Research Letters*, *39*. https://doi.org/10.1029/2012gl051886

Reynolds, C. S., Oliver, R. L., & Walsby, A. E. (1987). Cyanobacterial dominance: The role of buoyancy regulation in dynamic lake environments. *New Zealand Journal of Marine & Freshwater Research*, *21*, 379–390. https://doi.org/10.1080/00288330.1987.9516234

Rücker, J., Wiedner, C., & Zippel, P. (1997). Factors controlling the dominance of *Planktothrix agardhii* and *Limnothrix redekei* in eutrophic shallow lakes. In L. Kufel, A. Prejs, & J. I. Rybak (Eds.), *Shallow lakes '95. Developments in hydrobiology, 119*. Springer. https://doi.org/10.1007/978-94-011-5648-6_12

Ruddick, B., Anis, A., & Thompson, K. (2000). Maximum likelihood spectral fitting: The Batchelor Spectrum. *Journal of Atmospheric and Oceanic Technology*, *17*, 1541–1555. https://doi.org/10.1175/1520-0426(2000)017<1541:MLSFTB>2.0.CO;2

Saber, A., James, D. E., & Hayes, D. F. (2018). Effects of seasonal fluctuations of surface heat flux and wind stress on mixing and vertical diffusivity of water column in deep lakes. *Advances in Water Resources*, *119*, 150–163. https://doi.10.1016/j.advwatres.2018.07.006

Simoncelli, S., Thackery, S. J., & Wain, D. J. (2018). On biogenic turbulence production and mixing from vertically migrating zooplankton in lakes. *Aquatic Sciences*, *80*, 35. https://doi.org/10.1007/s00027-018-0586-z

Slavin, E. I. (2021). *Using artificial circulation for in-reservoir management of cyanobacteria and taste and odour metabolite production* (Doctoral thesis). University of Bath. https://researchportal.bath.ac.uk/en/studentTheses/using-artificial-circulation-for-in-reservoir-management-of-cyano

Stepanenko, V. M., Martynov, A., Jöhnk, K. D., Subin, Z. M., Perroud, M., Fang, X., et al. (2013). A one-dimensional model intercomparison study of thermal regime of a shallow, turbid midlatitude lake. *Geoscientific Model Development*, *6*, 1337–1352. https://doi.org/10.5194/gmd-6-1337-2013

Terry, J. A., Sadeghian, A., & Lindenschmidt, K.-E. (2017). Modelling dissolved oxygen/sediment oxygen demand under ice in a shallow eutrophic prairie reservoir. *Water*, *9*(2), 131. https://doi.org/10.3390/w9020131

Upadhyay, S., Bierlein, K. A., Little, J. C., Burch, M. D., Elam, K. P., & Brookes, J. D. (2013). Mixing potential of a surface-mounted solar-powered water mixer (SWM) for controlling cyanobacterial blooms. *Ecological Engineering*, *61*, 245–250. https://doi.org/10.1016/j.ecoleng.2013.09.032

Victoria State Government (2015). Biovolume calculator. Retrieved from https://www.water.vic.gov.au/__data/assets/excel_doc/0027/65592/BIOVOLUME-CALCULATOR.XLSX

Visser, P. M., Ibelings, B. W., Bormans, M., & Huisman, J. (2016). Artificial mixing to control cyanobacterial blooms: A review. *Aquatic Ecology*, *50*, 423–444. https://doi.org/10.1007/s10452-015-9537-0

Wagner, K. J. (2015). *Oxygenation and circulation to aid water supply reservoir management*. Water Resource Foundation.

Walsby, A. E., & Holland, D. P. (2006). Sinking velocities of phytoplankton measured on a stable density gradient by laser scanning. *Journal of The Royal Society Interface*, *3*, 429–439. https://doi.org/10.1098/rsif.2005.0106

Wang, Z., Huang, S., & Li, D. (2019). Decomposition of cyanobacterial bloom contributes to the formation and distribution of iron-bound phosphorus (Fe-P): Insight for cycling mechanism of internal phosphorus loading. *Science of the Total Environment*, *652*, 696–708. https://doi.org/10.1016/j.scitotenv.2018.10.260

Wanninkhof, R., Ledwell, J. R., & Crucius, J. (1991). *Gas transfer velocities on lakes measured with sulfur hexafluoride*. In S. C., Wilhelms, & J. S., Gulliver (Eds.), Proceedings of the second international symposium on gas transfer at water surfaces (pp. 441–455). American Society of Civil Engineers.

WEARS Australia. (2019). ResMix 1000. Retrieved from https://www.wears.com.au/resmix-product-range/resmix-1000-2/. 14 December 2019.

Wetzel, R. G. (1983). *Limnology* (2nd ed.). Saunders College Publishing.

Wetzel, R. G. (2001). *Limnology* (3rd ed.). Academic Press.

Woolway, R. I., Jones, I. D., Hamilton, D. P., Maberly, S. C., Muraoka, K., Read, J. S., et al. (2015). Automated calculation of surface energy fluxes with high-frequency lake buoy data. *Environmental Modelling & Software*, *70*, 191–198. https://doi.org/10.1016/j.envsoft.2015.04.013

Wüest, A., & Lorke, A. (2003). Small scale hydrodynamics in lakes. *Annual Review of Fluid Mechanics*, *35*, 373–412. https://doi.org/10.1146/annurev.fluid.35.101101.161220

Yang, Y., Wang, Y., Zhang, Z., Wang, W., Ren, X., Gao, Y., et al. (2018). Diurnal and Seasonal variations of thermal stratification and vertical mixing in a shallow freshwater lake. *Journal of Meteorological Research*, *32*, 219–232. https://doi.org/10.1007/s13351-018-7099-5

You, B.-S., Zhong, J.-C., Fan, C.-X., Wang, T.-C., Zhang, L., & Ding, S.-M. (2007). Effects of hydrodynamics on phosphorus fluxes from sediment in large, shallow Taihu Lake. *Journal of Environmental Sciences*, *19*, 1055–1060. https://doi.org/10.1016/S1001-0742(07)60172-7

YSI. (2020). EXO User Manual, [Online]. Retrieved from https://www.ysi.com/file%20library/documents/manuals/exo-user-manual-web.pdf